2022 Update for the Differences Between Thermodynamic Temperature and ITS-90 Below 335 K (F)

(iD) Christof Gaiser, (iD) Bernd Fellmuth, (iD) Roberto M. Gavioso, et al.

COLLECTIONS

Paper published as part of the special topic on Fundamental Constants: Realization of the Kelvin

(F)   This paper was selected as Featured

View Online   Export Citation   CrossMark

ARTICLES YOU MAY BE INTERESTED IN

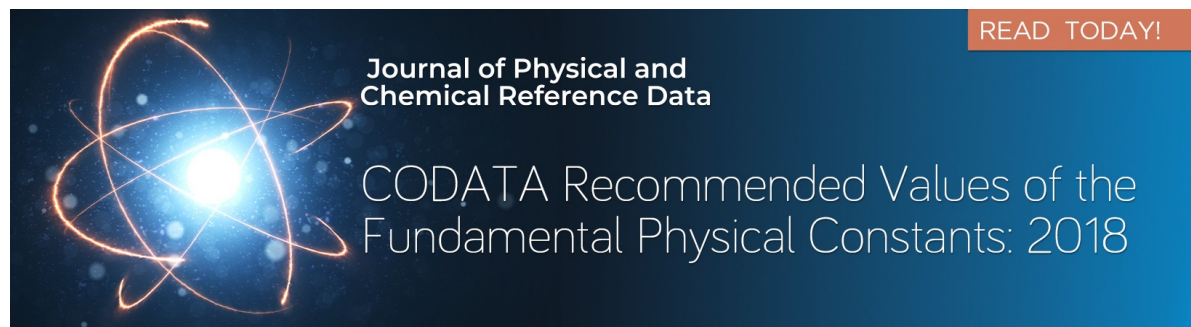A Fundamental Equation of State for the Calculation of Thermodynamic Properties of n-Octane
Journal of Physical and Chemical Reference Data **51**, 043103 (2022); https://doi.org/10.1063/5.0104661

Recent progress in oxidation behavior of high-entropy alloys: A review
APL Materials **10**, 120701 (2022); https://doi.org/10.1063/5.0116605

Electronic measurements of entropy in meso- and nanoscale systems
Chemical Physics Reviews **3**, 041308 (2022); https://doi.org/10.1063/5.0101784

Journal of Physical and Chemical Reference Data

READ TODAY!

CODATA Recommended Values of the Fundamental Physical Constants: 2018

2022 Update for the Differences Between Thermodynamic Temperature and ITS-90 Below 335 K (F)

Christof Gaiser,[1,a] (iD) Bernd Fellmuth,[1] (iD) Roberto M. Gavioso,[2] (iD) Murat Kalemci,[3] (iD) Vladimir Kytin,[4] (iD)
Tohru Nakano,[5] (iD) Anatolii Pokhodun,[6] (iD) Patrick M. C. Rourke,[7] (iD) Richard Rusby,[8] (iD) Fernando Sparasci,[9] (iD)
Peter P. M. Steur,[2] (iD) Weston L. Tew,[10] (iD) Robin Underwood,[8] (iD) Rod White,[11,b] (iD) Inseok Yang,[12] (iD)
and Jintao Zhang[13] (iD)

AFFILIATIONS

[1]Physikalisch-Technische Bundesanstalt (PTB), Abbestrasse 2-12, 10587 Berlin, Germany

[2]Istituto Nazionale di Ricerca Metrologica (INRiM), Strada Delle Cacce 91, 10135 Torino, Italy

[3]TÜBİTAK UME (UME), Gebze Yerleşkesi P.K. 54, 41470 Gebze, Kocaeli, Turkey

[4]All-Russian Research Institute of Physical Technical and Radio Technical Measurements (VNIIFTRI) Mendeleevo,
Solnechnogorsky District, 141570 Moscow Region, Russia

[5]National Metrology Institute of Japan (NMIJ, AIST), Tsukuba Central 3, 1-1-1 Umezono, Tsukuba, Ibaraki 305-8563, Japan

[6]D. I. Mendeleyev Institute for Metrology (VNIIM), Moskovsky pr., 19, 190005 St. Petersburg, Russia

[7]National Research Council Canada (NRC), 1200 Montreal Road, Ottawa, Ontario K1A 0R6, Canada

[8]National Physical Laboratory (NPL), Hampton Road, TW11 0LW Teddington, United Kingdom

[9]Laboratoire Commun de Métrologie (LNE-CNAM), 61 Rue Du Landy, 93210 La Plaine-Saint-Denis, France

[10]National Institute of Standards and Technology (NIST), 100 Bureau Dr., Gaithersburg, Maryland 20899, USA

[11]Measurement Standards Laboratory (MSL), 69 Gracefield Road, Lower Hutt 5010, New Zealand

[12]Korea Research Institute of Standards and Science (KRISS), Daejeon 34113, South Korea

[13]National Institute of Metrology (NIM), Beijing 100029, People's Republic of China

Note: This paper is part of the Special Topic, Fundamental Constants: Realization of the Kelvin.
[a]Author to whom correspondence should be addressed: christof.gaiser@ptb.de
[b]Retired.

ABSTRACT

In 2011, a working group of the Consultative Committee for Thermometry published their best estimates of the differences between the thermodynamic temperature T and its approximation (T_{90}), the temperature according to the International Temperature Scale of 1990, ITS-90. These consensus estimates, in combination with measurements made in accordance with ITS-90, are an important alternative to primary thermometry for those requiring accurate measurements of thermodynamic temperature. Since 2011, there has been a change in the definition of the kelvin and significant improvements in primary thermometry. This paper updates the ($T - T_{90}$) estimates by combining and analyzing the data used for the 2011 estimates and data from more recent primary thermometry. The results of the analysis are presented as a 12th-order polynomial representing the updated consensus values for the differences and a sixth-order polynomial for their uncertainty estimates.

© 2022 Author(s). All article content, except where otherwise noted, is licensed under a Creative Commons Attribution (CC BY) license (http://creativecommons.org/licenses/by/4.0/). https://doi.org/10.1063/5.0131026

Key words: thermodynamic temperature; primary thermometry; international temperature scale; ITS-90; gas thermometry.

CONTENTS

List of Tables

List of Figures

1. Introduction

On 20 May 2019, four of the base units of the International System of Units (SI) were redefined by fixing the values of four fundamental physical constants.[1,2] Among these, the base unit of thermodynamic temperature has been defined by fixing the value of the Boltzmann constant, rather than by fixing the temperature of a particular state of matter.[3] The new definition eliminates the uncertainty in the realization of the triple point of water from the realization of the kelvin and encourages direct realization of the kelvin using any thermodynamic method appropriate for the temperature of interest. In the *mise en pratique* for the kelvin (MeP-K), the Consultative Committee for Thermometry (CCT) identifies the primary methods that are both well documented and achieve state-of-the-art uncertainties.[4,5] Primary methods are especially important for scientific purposes.

However, primary methods are not suited to routine thermometry: all require a high level of expertise, and most are very slow and require expensive, often custom-built equipment. Additionally, primary methods have historically had unacceptably high measurement uncertainties.[3] The solution has been for the International Committee for Weights and Measures (CIPM) to define more practical International Temperature Scales (ITS) approximating thermodynamic temperatures using defined reference temperatures and interpolating thermometers. The International Temperature Scale of 1990, ITS-90,[6] is the current basis for internationally consistent temperature measurements, denoted as T_{90}, and defines scale temperatures from 0.65 K up to the highest measurable temperatures. The uncertainty of its realization ranges from a few tenths of a millikelvin below 335 K and increases to several millikelvin at 1225 K.[7] ITS-90 was defined so that the scale temperatures, T_{90}, corresponded closely to the known thermodynamic temperatures, T, at the time of definition.

As primary methods improve, the differences between T and T_{90} become increasingly apparent. In 2011, CCT Working Group 4 published the then best estimates of the differences $(T - T_{90})$.[8] This paper is the basis for the CCT guide "*Estimates of the Differences between Thermodynamic Temperature and the ITS-90.*"[9] The use of ITS-90 combined with knowledge of $T - T_{90}$ is an important alternative to primary thermometry.

Since 2011, several primary methods have undergone significant improvements accompanying research undertaken to determine the Boltzmann constant for the redefinition of the kelvin.[10,11] Subsequently, the improved methods have been used to measure $T - T_{90}$ over temperatures ranging from 4 to 323 K. The CCT Working Group for Contact Thermometry (CCT-WG-CTh) has now collated the new data and combined them with those published in Ref. 8 to update the best estimates of $(T - T_{90})$.

The data used in the analysis are presented in Sec. 2. Section 3 then identifies a polynomial representation of $(T - T_{90})$ versus T_{90} and summarizes the considerations in its development. Section 4 discusses uncertainties associated with the estimates of $(T - T_{90})$ and how they are to be applied. Finally, Sec. 5 summarizes the results and conclusions.

2. Overview of Literature Data

For the 2011 estimates, the input data and the uncertainties were provided by the researchers in polynomial form and evaluated at the temperatures listed in Table 1. The various researchers have taken responsibility for the use of these values. Especially in the case of the data published before 1990, corrections were required for the change in scale from IPTS-68,[6] and some uncertainties required harmonization following the publication of the Guide to the Expression of Uncertainty in Measurement

TABLE 1. $(T - T_{90})$ input data together with uncertainty estimates. The references are given in the left column. The uncertainty values marked with an asterisk are the ones used for estimating u_{minexp} shown in Fig. 3. For a complete reproduction of the values published in Ref. 8, dataset PTB_2011_org listed in Table 5 of the Appendix must be used (for details, see footnotes a and b)

	T_{90} (K)	$(T - T_{90})$ (mK)	$u(T - T_{90})$ (mK)
Since 2019[a]	273.16	0.00	0.10
VNIIFTRI_2011[22]	4.2	0.02	0.40
	5	−0.08	0.42
	6	−0.16	0.44
	7	−0.20	0.46
	8	−0.20	0.48
	9.288	−0.16	0.51
	11	−0.05	0.54
	13.8033	0.17	0.61
	17.035	0.36	0.68
	20.27	0.35	0.75
	22.5	0.18	0.80
	24.5561	−0.21	0.84
	35	−0.62	1.07
	45	−0.14	1.29
	54.3584	0.40	1.50
	70	0.52	1.82
	77.657	0.04	1.97
	83.8058	−0.60	2.09
	90	−1.46	2.19
	100	−3.20	2.35
	130	−9.04	2.67
	161.405	−11.57	2.68
	195	−7.65	2.32
	234.3156	−0.42	1.61
	255	0.81	1.30
	290	0.08	1.40
	302.9146	3.04	1.81
INRIM_2011[13]	234.3156	−2.95	0.91
	255	−2.01	0.90
	290	1.61	0.96
	302.9146	3.26	1.01
	335	7.23	1.21
NPL_2011[26]	4.2	0.00	0.20
	5	0.04	0.21
	6	0.09	0.22
	7	0.14	0.23
	8	0.18	0.25
	9.288	0.23	0.27
	11	0.28	0.30
	13.8033	0.33	0.34
	17.035	0.35	0.37
	20.27	0.32	0.40
	22.5	0.27	0.43
	24.5561	0.21	0.48

TABLE 1. (*Continued*)

	T_{90} (K)	$(T - T_{90})$ (mK)	$u(T - T_{90})$ (mK)
PTB_2011_rev[21]	4.2	−0.07	0.23
	5	0.03	0.18
	6	0.09	0.19
	7	0.07	0.19
	8	0.03	0.20
	9.288	−0.01	0.21
	11	0.03	0.22
	13.8033	0.20	0.24
	17.035	0.25	0.27
	20.27	0.12	0.30
	22.5	0.08	0.31
	24.5561	0.03	0.31
UL-ICL_2011[18]	90	−7.29	1.02
	100	−7.74	1.00
	130	−8.49	0.94
	161.405	−8.33	0.93
	195	−7.11	0.95
	234.3156	−4.28	1.04
	255	−2.18	1.11
	290	1.78	1.26
NML_2011[25]	17.035	−0.70	1.12
	20.27	−0.35	1.29
	22.5	−0.14	1.40
	24.5561	0.03	1.49
	35	0.63	1.97
	45	0.85	2.39
	54.3584	0.82	2.74
	70	0.46	3.25
	77.657	0.20	3.47
	83.8058	−0.02	3.62
	90	−0.26	3.76
	100	−0.64	3.96
	130	−1.55	4.31
	161.405	−2.00	4.29
	195	−2.00	3.83
	234.3156	−1.59	2.72
	255	−1.05	1.88
KOL_2011 based on Ref. 23	4.2	−0.57	0.48
	5	−0.25	0.50
	6	−0.46	0.52
	7	−0.47	0.54
	8	−0.36	0.56
	9.288	−0.37	0.59
	11	−0.69	0.63
	13.8033	−0.70	0.70
	17.035	−0.24	0.80
	20.27	−0.59	0.90
	22.5	−0.87	0.97
	24.5561	−1.34	1.05
	35	−1.70	1.48
	45	−2.35	1.98
	54.3584	−2.93	2.54

TABLE 1. (*Continued*)

	T_{90} (K)	$(T - T_{90})$ (mK)	$u(T - T_{90})$ (mK)
	70	−3.66	3.63
	77.657	−3.84	4.24
	83.8058	−4.10	4.77
	90	−5.03	5.34
	100	−6.19	6.33
	234.3156	−3.33	0.60
	255	−2.08	0.60
NIST_2011[15–17]	290	2.81	0.56
	302.9146	4.58	0.57
	335	7.72	0.60
	7	−0.14	0.12
	8	0.01	0.13
	9.288	0.20	0.15
	11	0.43	0.17
	13.8033	0.72	0.21
	17.035	0.80	0.25
	20.27	0.46	0.29
	22.5	−0.10	0.32
LNE_NIST_2011[14]	24.5561	−0.90	0.35
	77.657	−3.98	0.37*
	83.8058	−4.58	0.40*
	90	−5.16	0.44*
	100	−6.04	0.48
	130	−7.98	0.60
	161.405	−8.44	0.68
	195	−7.00	0.70
	234.3156	−3.48	0.67
	255	−1.45	0.62
	4.2	−0.22	0.64
	5	−0.05	0.67
	6	0.14	0.71
	7	0.31	0.76
	8	0.46	0.80
	9.288	0.62	0.84
NMIJ_2011[24]	11	0.78	0.89
	13.8033	0.90	0.91
	17.035	0.83	0.84
	20.27	0.52	0.73
	22.5	0.18	0.66
	24.5561	−0.23	0.64

[a]In 2011, $T - T_{90} = 0$ mK with $u(T - T_{90}) = 0$; after the redefinition of the kelvin, still $T - T_{90} = 0$ mK, but now, $u(T - T_{90}) = 0.10$ mK, temperature equivalent to the uncertainty of the Boltzmann constant right before its redefinition.

[b]To reproduce the numbers given in Table 2 of Ref. 8, the following information is needed. Between 4.2 and 24.5 K and from 290 up to 335 K (and above), simple weighted means of the tabulated values and the associated uncertainties were calculated (for the PTB data, the original data given in Table 5 of the Appendix were used). [At 303 K, a double counting of one dataset in the evaluation of Ref. 8 led to a slightly different value (the correct value at 303 K would have been $(T - T_{90}) = 4.18$ mK with an uncertainty of 0.48 mK).] From 35 to 70 K, the so-called BOB method (the name comes from Type B on bias; see Sec. 4 in Ref. 57) and the associated uncertainty were used. From 77 to 255 K, the weighted mean was calculated, and its uncertainty was multiplied by a factor according to Student's distribution ($k = 2$), considering the individual degrees of freedom at the specific temperature.

(GUM).[12] This review was carried out by WG4 in a process lasting more than five years. The corrected and harmonized data in Table 1 constitute the first part of the input for the present work (see footnote b below Table 1). It includes data from ten research groups using one of three primary methods:

- Acoustic Gas Thermometry (AGT): Istituto Nazionale di Ricerca Metrologica (INRIM) (polynomial based on data from Ref. 13), Laboratoire Commun de Métrologie (LNE)–National Institute of Standards and Technology (NIST) (polynomial based on data from Ref. 14), NIST (polynomial based on data from Refs. 15–17), and University of London (UL)–Imperial College London (ICL) (polynomial based on data from Ref. 18).
- Dielectric-Constant Gas Thermometry (DCGT): Physikalisch-Technische Bundesanstalt (PTB) [in Ref. 8, a polynomial based on data from Refs. 19 and 20 was used (see Table 5 in the Appendix); these data were revised in Ref. 21 due to systematic changes in the compressibility values of the capacitors; in Table 1, therefore, the revised values from Ref. 21 are listed; in view of the large amount of data points, only 12 of 22 measuring temperatures between 4 and 25 K given in Ref. 21 are used; the interpolation between the points and uncertainties was performed via cubic splines].
- Constant-Volume Gas Thermometry (CVGT): All-Russian Research Institute of Physical Technical and Radio Technical Measurements (VNIIFTRI) (polynomial based on data from Ref. 22), Kamerlingh Onnes Laboratory (KOL) (polynomial based on data from Ref. 23 recalculated and agreed by WG4 at that time to interpolate the thermodynamic data in ranges with very few data points. The shift of the original KOL data[23] was significant but always compatible with the uncertainty estimated by WG4 as given in Table 1), National Metrology Institute of Japan (NMIJ) (polynomial based on data from Ref. 24), National Measurement Laboratory (NML) (polynomial based on data from Ref. 25), and National Physical Laboratory (NPL) (polynomial based on data from Ref. 26).

The data measured after 2011 and the related uncertainties are given in Table 2. The new results are from eight research groups using one of four primary methods:

- AGT: INRIM (Table 1 in Ref. 27), National Institute of Metrology (NIM) (Tables 14 and 15 in Ref. 28), NPL (Table 1 in Ref. 29), VNIIFTRI (Abstract in Ref. 30), LNE–Technical Institute of Physics and Chemistry (TIPC) (Table 1 in Ref. 31; the values are not explicitly stated but obvious), and NMIJ (Table 1 in Ref. 32).
- DCGT: PTB (Table 2 in Ref. 21, Table 2 in Ref. 33, and Table 2 in Ref. 34).
- Refractive-Index Gas Thermometry (RIGT): National Research Council Canada (NRC) (Abstract in Ref. 35), INRIM (Table 1 in Corrigendum[36]), and TIPC-LNE (Table 9 in Corrigendum[37]).
- CVGT: NMIJ (Fig. 4 in Ref. 38; the data in Table 2 of the present publication are a private communication).

TABLE 2. $(T - T_{90})$ input data together with uncertainty estimates. The references are given in the left column. The data points highlighted in bold are the ones used for the reduced dataset (see Fig. 4). The uncertainty values marked with an asterisk are the ones used for estimating u_{minexp} shown in Fig. 3

	T_{90} (K)	$(T - T_{90})$ (mK)	$u(T - T_{90})$ (mK)
	5.000 21	0.33	0.1*
	6.000 06	0.4	0.11*
	7.000 26	0.37	0.1*
	8.000 97	0.3	0.11*
	10.000 94	0.24	0.13*
	12.000 52	0.37	0.13*
	13.804 28	0.62	0.16*
	15.000 62	0.76	0.19
TIPC-LNE[36]	**16.000 12**	0.81	0.22
	17.033 89	0.79	0.22
	17.999 77	0.7	0.22*
	18.998 73	0.56	0.21
	20.267 9	0.28	0.19*
	20.998 28	0.15	0.2
	21.999 73	−0.05	0.22*
	23.000 25	−0.21	0.25
	24.555 35	−0.35	0.26
LNE-TIPC[31]	24.556 1	−0.95	0.24*
	13.803 3	0.75	1.7
	24.556 1	−1.11	0.39
	54.358 4	−3.44	0.53
	83.805 8	−4.35	1.05
INRIM[27,36]	**161.406**	−6.37	2.9
	236.619	−2.43	0.34
	247	−2.65	0.25
	260.12	−1.58	0.29
	302.914 6	3.73	0.33
	334.17	6.57	0.42*
	234.210 7	−1.8	0.5
	243.105 1	−3.3	0.5
NIM[28]	**258.078**	−0.6	0.5
	292.693 7	2.1	0.6
	298.227 2	2.4	0.7
	303.261 4	3.7	0.8
	4.221 94	0.10	0.7
	4.590 18	0.19	0.7
	5.002 27	0.27	0.7
	5.470 85	0.35	0.7
	6.001 47	0.47	0.8
	6.599 57	0.57	0.8
	7.302 68	0.68	0.8
	8.103 5	0.80	0.9
	10.001	1.00	0.9
NMIJ[32,38]	12.001 1	1.12	1
	13.804 4	1.14	0.9
	15.419 7	1.09	0.9
	17.036	0.99	0.9
	18.646 1	0.83	0.8

TABLE 2. (*Continued*)

	T_{90} (K)	$(T - T_{90})$ (mK)	$u(T - T_{90})$ (mK)
	20.270 6	0.61	0.7
	22.300 2	0.25	0.7
	24.555 9	−0.23	0.6
	283.15	1.3	0.7
	293.15	2.7	0.8
	302.914 6	4.1	0.8
	118.15	−6.27	0.42
	133.15	−7.08	0.44*
	148.15	−7.5	0.44
	163.15	−7.08	0.42*
	178.15	−5.94	0.39
	191.15	−4.76	0.36*
	207.15	−3.46	0.34
	223.15	−3.08	0.26
	233.15	−2.83	0.23*
	243.15	−2.73	0.21
	253.15	−2.26	0.19*
NPL[29]	**258.15**	−1.86	0.21
	263.15	−1.29	0.2
	268.15	−0.94	0.2
	278.15	0.77	0.18
	283.15	1.32	0.21
	288.15	2.06	0.25*
	293.15	2.70	0.28
	298.15	3.24	0.32
	303.15	3.79	0.32*
	313.15	5.00	0.43
	323.15	5.68	0.51
	24.556 1	−0.61	0.49
NRC[35]	**54.358 4**	−2.0	0.8
	83.805 8	−4.1	1.6
	161.405 96	−6.9	1.7
	3.998 31	0.12	0.21*
	13.764 66	0.07	0.25
	24.555 18	−0.56	0.28
	28.5	−0.23	0.45
	30	−0.25	0.50
	30	−0.76	0.78
	31.5	−0.25	0.52
	32	−0.46	0.55
	33	−0.24	0.52
	34	−0.87	0.41*
	34.5	−0.24	0.52
	36	−0.95	0.42
PTB[21,33,34]	36	−0.26	0.52
	38	−0.86	0.63
	49.835 01	−1.86	0.30*
	50.786 863	−1.93	0.27
	59.784 505	−2.11	0.31*
	69.738 738	−3.09	0.39*
	78.558 011	−3.82	0.42

TABLE 2. (Continued)

	T_{90} (K)	$(T - T_{90})$ (mK)	$u(T - T_{90})$ (mK)
	84	−3.74	0.43
	100.495 53	−5.16	0.48*
	120	−5.06	0.65
	130	−7.21	1.57
	140	−6.15	1.67
	200.087 84	−4.40	0.99
VNIIFTRI[30]	79	−4.47	0.97
	83.805 8	−4.81	1.02

The previous definition of the kelvin fixed the temperature of the triple point of water (TPW), T_{TPW}, to 273.16 K with zero uncertainty so that $(T - T_{90})_{TPW}$ was identically zero. This was reflected in the 2011 estimates in which the least-squares fit and uncertainty were forced to zero at the TPW.[8]

On 20 May 2019, the new definition of the kelvin took effect, and the Boltzmann constant was fixed to the final CODATA adjusted value with zero uncertainty.[1,39] Although T_{TPW} remained 273.16 K at the moment of redefinition, it acquired an uncertainty of 0.1 mK transferred from the Boltzmann constant experiments, and it is no longer fixed. A corresponding data point $(T - T_{90})_{TPW}$ = 0.0(1) mK is included in the fitted data, and the $D(T_{90})$ polynomial fit to the $(T - T_{90})$ data, see Sec. 3, has not been forced to zero at the TPW. This reflects the fact that the value of T_{TPW} is no longer fixed by definition.

3. Fitting-Function Selection and Tests

The aim of the analysis is to develop a smooth analytic function, $D(T_{90})$, describing the best estimate of $T - T_{90}$ as a function of the measured scale temperature, T_{90}. Ideally, the function should cover the full range of the data, 4–323 K, and achieve the best compromise in capturing the underlying structure of the data while not exhibiting excessive sensitivity to measurement errors, i.e., overfitting. In the temperature range of interest, all data (including those used to establish ITS-90) were obtained with various types of gas thermometers for which all the known forms of measurement errors are free of asymptotic or exponential effects that might cause discontinuities or other difficult-to-fit artifacts in the data. Therefore, there was a reasonable expectation that a fitted function based on a power series with linear coefficients would be both satisfactory and the simplest choice,

$$D(T_{90})/\text{mK} = (T - T_{90})/\text{mK} = \sum_{i=0}^{n} a_i (T_{90}/\text{K})^i. \quad (1)$$

It was the consensus of CCT-WG-CTh that all data listed in Tables 1 and 2 were fitted together. The least-squares software used for the analysis employs Björck's orthonormal modification of the Gram–Schmidt algorithm,[40,41] which minimizes the effects of round-off errors in the numerical computations. To confirm the correct operation of the software, the computations were checked using a generalized nonlinear least-squares application written

by Saunders[42,43] employing the iterative Levenberg–Marquardt algorithm.[44] Saunders' application was also used to calculate the propagated uncertainties and in numerical experiments, evaluating the effects of correlations. An important benefit of the Björck algorithm is that the polynomials are orthonormal in the set of arguments (set of independent variables). The use of orthogonal functions has the advantage that the coefficients are independent of each other. Furthermore, their magnitude allows for a rigorous but simple test for the selection of an appropriate fitting order. This selection is an important task since one must avoid the extremes of too high an order with a resultant overfit and unrepresentative oscillations or too low an order with a resultant underfit and loss of experimental information. The left part of Fig. 1 shows the natural logarithm of the absolute values of the orthogonal coefficients obtained with the Björck algorithm for data listed in Tables 1 and 2, in dependence on the fitting order. If the fitting functions are necessary for describing the data (called "true or signal functions" in Ref. 45), there is a tendency of decreasing absolute value, i.e., the coefficients converge. However, the coefficients of further unnecessary ("noise") functions show no tendency to converge. From Fig. 1, it can, therefore, be concluded that order 11 or 12 may be sufficient.

One further traditional statistical test for the quality of a least-squares fit is the chi-square test. If all the uncertainty estimates, u_i, are correct and the measurement errors are independent and normally distributed, the weighted least-squares sum minimized by the software,

$$\chi^2 = \sum_{i=1}^{N} \frac{[(T - T_{90})_i - D(T_{90})]^2}{u_i^2}, \quad (2)$$

is a sample drawn from a chi-square distribution with N being the number of data points.

Typically, the calculated χ^2 value falls as the order of the fit increases and converges to a constant value when there is no more structure to be detected in the data. If the asymptotic value for χ^2 is too large or too small, then one or more of the assumptions is incorrect. Figure 2 shows that the residuals to the weighted fit are very nearly normally distributed, and the χ^2 value calculated from the fits of order larger than 10 to the combined data of Tables 1 and 2 is also within expected bounds. While the chi-square test is a useful indicator confirming that a model is consistent with measurement uncertainties, it is not a discerning test of fit order.

Two commonly used tests for the quality of fit are based on the Bayesian Information Criterion (BIC) and the Akaike Information Criterion with the small-number correction (AICc) (for details, see Ref. 46). For a weighted least-squares fit using normally distributed data with correctly estimated uncertainties, both the AICc and the BIC for an nth-order polynomial can be expressed as

$$BIC = k \ln(N) + \chi^2 \quad (3)$$

and

$$AICc = 2k + \frac{2k(k+1)}{N - k - 1} + \chi^2 \quad (4)$$
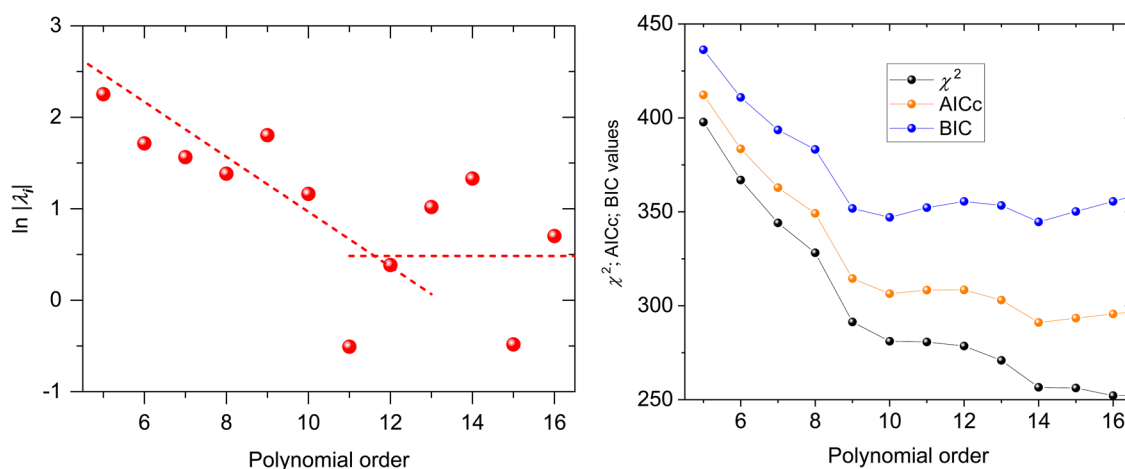
with $k = n + 2$.

FIG. 1. Left: Natural logarithm of the absolute values of the orthogonal coefficients λ_i, obtained by fitting power series to the $(T - T_{90})$ data listed in Tables 1 and 2 applying the Björck algorithm, in dependence on the fitting order. The dashed lines are a line fit to the steep part of the data and a fit of a constant to the flat part of the data, respectively. Their intersection suggests a 11th- or 12th-order fit. Right: Statistical measures for fit quality vs polynomial order: χ^2, AICc, and BIC (for details, see the text).

The right part of Fig. 1 plots the values of χ^2, AICc, and BIC versus the fit order, n. The optimum fit order is identified by the minimum of the curves. There is a subtle difference between the two criteria. Ideally, the minimum of the BIC identifies the model that is the best descriptor of the analyzed data, whereas the minimum of the AICc identifies the model that is the best predictor of new data. Since the polynomial is to be used to correct new temperature measurements, the AICc is the appropriate measure of fit quality. It suggests that any polynomial in the range 10th to 14th order would be similarly satisfactory. The BIC and AICc tests are comparative measures, but they do not indicate that we have found the best of all possible models. Therefore, there is still a requirement for the model to be reasonable and to fit the data well. In addition to the evidence from the χ^2 value and the distribution of residuals showing that the model is reasonable, a visual inspection of the data and the

fitted polynomials showed that there was little difference among all models of 11th order and above, except for a small "bulge" in the residuals near 320 K, which largely disappeared with the 12th-order model.

To test for hidden uncertainty components due to the use of different primary thermometers, the datasets listed in Tables 1 and 2 were allocated in three groups. The first one is the CVGT group, the second one is the AGT group, and the third one is the PGT group, which combines data from both DCGT and RIGT. A separate study of DCGT and RIGT is not reasonable due to the similarity of the methods. The only difference is the detection technique, which is in the case of DCGT a capacitance measurement and in the case of RIGT a microwave frequency measurement. Therefore, both techniques have been merged to PGT (see MeP-K[4,5]). The three individual datasets have been treated in the same way as the complete dataset discussed before. The only difference is the use of fit order seven instead of 12 to avoid oscillations. The uncertainty estimates are simply the smallest uncertainties of individual experiments for the specific temperature range (marked with an asterisk in Tables 1 and 2). In Fig. 3, it is clearly shown that all primary thermometers agree well within their uncertainties. This is a strong argument that the datasets can be treated together as one dataset, and a splitting into individual primary thermometers is not necessary.

The following stability checks of the result have been made. The first test was performed with a reduced dataset, where the number of data points was almost halved. In particular, the most accurate data from Ref. 29 have been thinned out. The choice was random with the idea to demonstrate that the fit is not solely dominated by the data with the lowest uncertainty. The specific points used for the reduced dataset are marked in bold in Table 2. The next check was performed with an unweighted fit of 12th order to the complete dataset, and finally, a weighted ninth-order fit was made. All deviations relative to the weighted 12th-order full-data-set fit $D(T_{90})$ are shown in Fig. 4. It is clearly visible that the fitting result is extremely stable.
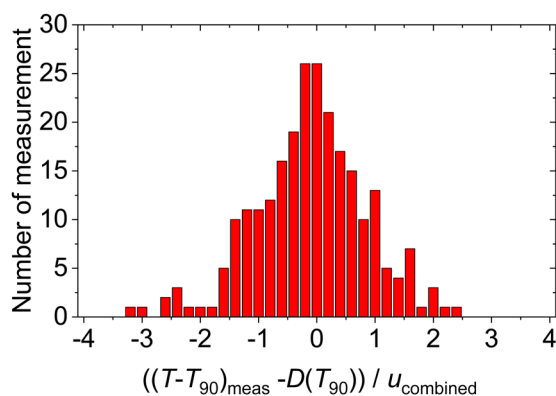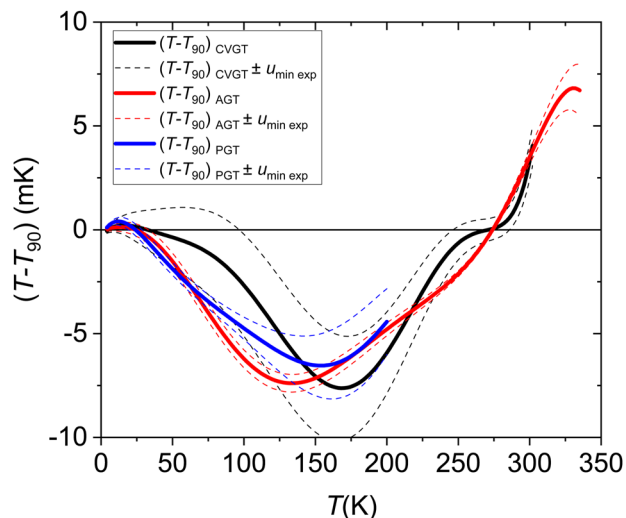

FIG. 2. Number of measurements versus the ratio of the deviation between the single experiment $(T - T_{90})_{meas}$ and $D(T_{90})$ to the combined uncertainty of the single experiment and $u[D(T_{90})]$, $u_{combined}$.

FIG. 3. The data listed in Tables 1 and 2 were allocated in datasets for the three primary thermometer types CVGT, AGT, and PGT (polarizing gas thermometry, PGT, combines DCGT and RIGT as defined in the MeP-K[4,5]). The results of weighted fits of seventh order in $(T - T_{90})$ versus temperature for the three primary thermometers are shown as solid lines. The thin dashed lines of specific color envelop the range $(T - T_{90}) \pm u_{minexp}$, with u_{minexp} corresponding to the minimal single-experiment standard uncertainty estimates and marked in Tables 1 and 2 by asterisks.

$D(T_{90})$ is neither dominated by the fit order nor, in most parts, by the weighting of a specific dataset. The reason for the larger deviation of the unweighted fit between 50 and 100 K is that most of data in this range have larger uncertainties and larger deviations from the overall fit. This has no effect on the weighted fit but leads to stronger
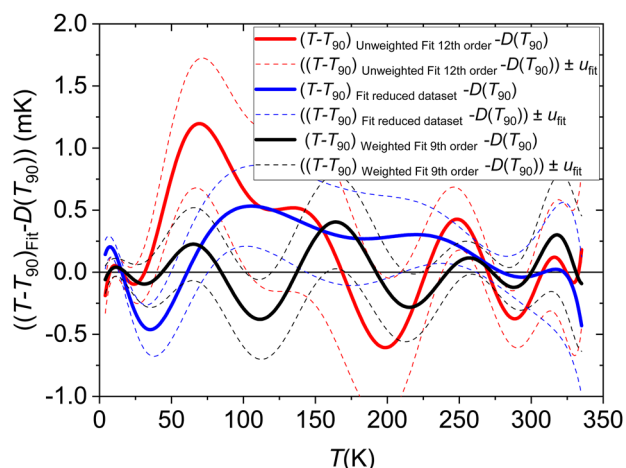

FIG. 4. Deviation of different fitting results from the function $D(T_{90})$ obtained by a weighted 12th-order fit: Blue line: reduced dataset (see the text). Red line: unweighted 12th-order fit of the complete dataset. Black line: weighted ninth-order fit. The thin dashed lines of specific color envelop $[(T - T_{90})_{fit} - D(T_{90})] \pm u_{fit}$, with the specific standard fitting uncertainty estimates u_{fit}.

TABLE 3. Fitting coefficients for the power series approximating the $(T - T_{90})$ input data $[D(T_{90})$: $\alpha_i]$ and its standard uncertainty estimates $\{u_{combined-LS}[D(T_{90})]$: $\beta_i\}$ resulting from a least-squares fit to $u_{combined}$ in specific temperature ranges, respectively

i	α_i	β_i
0	$-6.393\,509\,785 \times 10^{-1}$	$6.362\,639 \times 10^{-2}$
1	$2.044\,362\,025 \times 10^{-1}$	$1.251\,359 \times 10^{-2}$
2	$-1.453\,482\,491 \times 10^{-2}$	$-3.880\,108 \times 10^{-4}$
3	$4.860\,355\,653 \times 10^{-4}$	$4.878\,407 \times 10^{-6}$
4	$-1.152\,913\,045 \times 10^{-5}$	$-2.789\,077 \times 10^{-8}$
5	$1.932\,372\,065 \times 10^{-7}$	$7.268\,939 \times 10^{-11}$
6	$-2.222\,708\,123 \times 10^{-9}$	$-6.999\,818 \times 10^{-14}$
7	$1.722\,390\,583 \times 10^{-11}$	
8	$-8.878\,574\,513 \times 10^{-14}$	
9	$2.985\,516\,966 \times 10^{-16}$	
10	$-6.273\,436\,285 \times 10^{-19}$	
11	$7.467\,125\,710 \times 10^{-22}$	
12	$-3.840\,581\,614 \times 10^{-25}$	

unrealistic deviations for the unweighted fit. In other temperature ranges, this is not the case.

Finally, the 12th-order polynomial was chosen: the coefficients are given in Table 3, and the agreement between the fit function $D(T_{90})$ and the individual experimental data $(T - T_{90})_{meas}$ is analyzed as follows. Figure 2 plots a histogram of the normalized residuals of the fit $[(T - T_{90})_{meas} - D(T_{90})]/u_{combined}$, where $u_{combined}$ is the combined uncertainty of the fit and the uncertainties listed in Tables 1 and 2. Ideally, the normalized residuals should be normally distributed. The actual distribution is close to normal, perhaps very slightly skewed, and has most of the 219 points within ± 3, as expected. There are also no conspicuous outliers. In Fig. 5, the experimental data are plotted together with $D(T_{90})$, and in Fig. 6, the corresponding residuals are shown with a remarkable consistency between the residuals and the uncertainties. Evidently, the number of outliers is negligible, and their deviations are tolerable.

The fitted polynomial is continuous in all derivatives over the range of the data and has a slope at TPW of 0.132(6) mK K^{-1}. In contrast, the 2011 formulation of $D_{2011}(T_{90})$ used different analytical functions below and above TPW, with slopes of 0.070 mK K^{-1} (below TPW) and 0.101 mK K^{-1} (above TPW).[8] The steeper slope of the present work reflects the extra detail from new low-uncertainty acoustic gas thermometry measurements in the vicinity of the TPW.[27–29] No anomaly in thermodynamic temperature, T, is expected at TPW, but the scale temperature, T_{90}, has small discontinuities in the first and third derivatives due, respectively, to the different ITS-90 interpolating equations[3,47] and the different reference functions[48] below and above TPW.

4. Uncertainties

The two dashed lines in Fig. 6 plot the envelope of the standard uncertainty, $u[D(T_{90})]$, derived from three contributions. The first contribution, $u_{fit}[D(T_{90})]$, is propagated from the uncertainties reported in the data used in the least-squares fit (Tables 1 and 2).
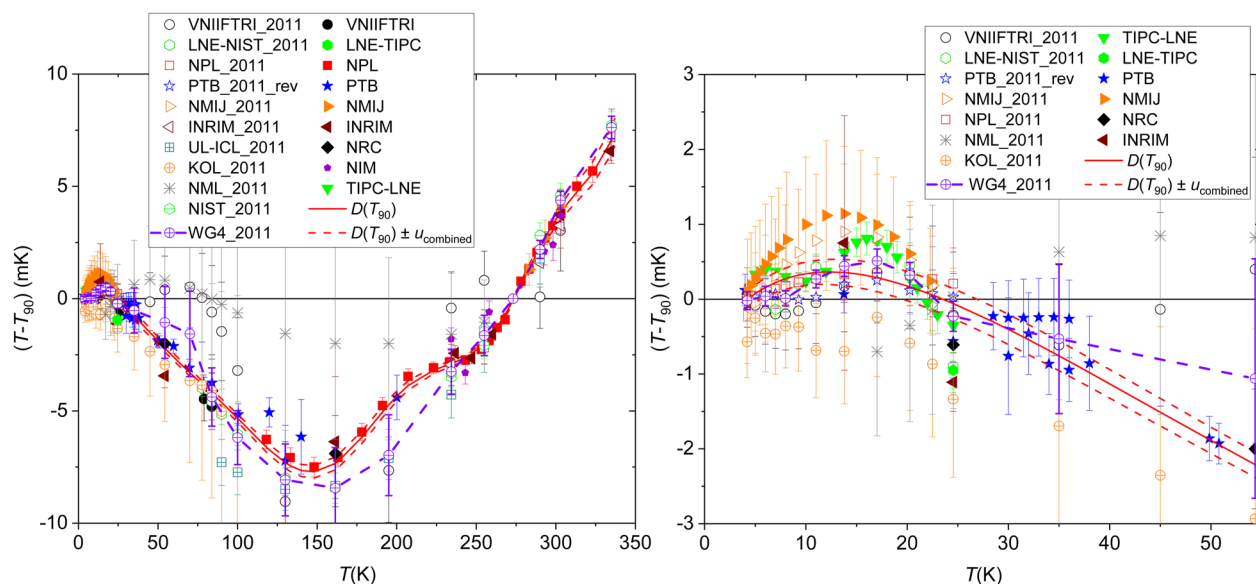
FIG. 5. Left: $(T - T_{90})$ data as listed in Tables 1 and 2 versus temperature T_{90}. The institutes at which the data have been obtained are listed in the legend. WG4 is the data contained in Table 2 of Ref. 8 and shown for comparison purposes. The red full line shows the fitting function $D(T_{90})$, and the dashed lines envelop the range $D(T_{90}) \pm u_{combined}[D(T_{90})]$ with the combined standard uncertainty $u_{combined}[D(T_{90})]$. Right: The same as on the left but in a restricted temperature range.

See Ref. 44 for the uncertainty propagation equations. The uncertainty propagation for weighted least-squares fits assumes that the weighted residuals in the fit are independent and identically distributed. As shown in Fig. 2, the residuals are very close to expectations. However, the patterns of residuals in Fig. 6 show that the residuals are not independent. Correlations in the residuals arise from small systematic effects within each dataset, including non-uniqueness in the realizations of ITS-90 used in each experiment.
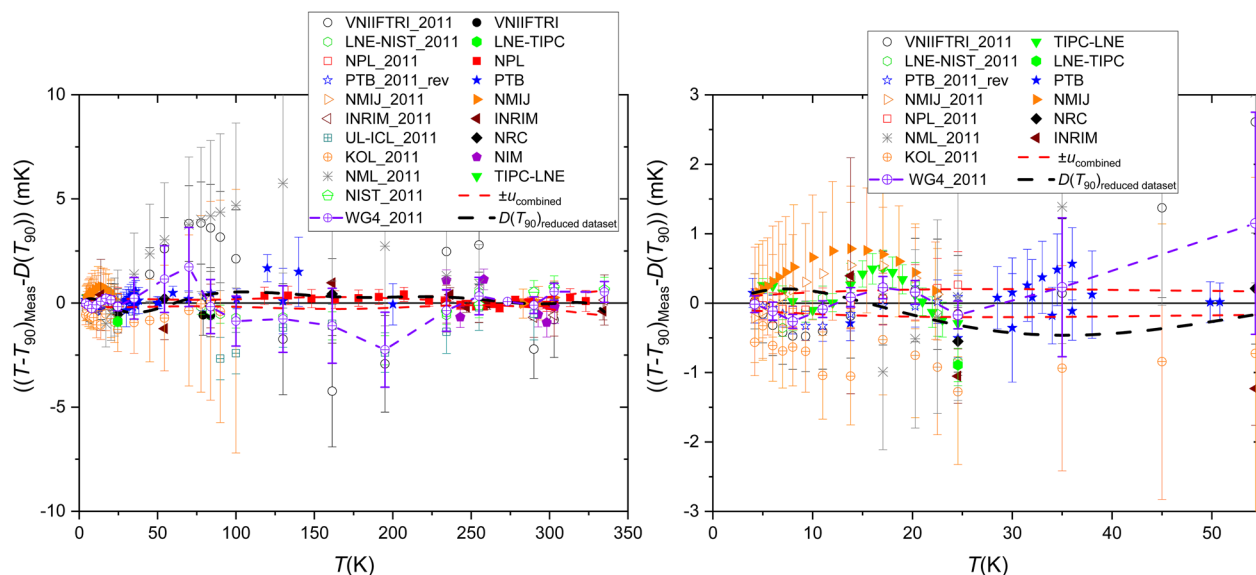
FIG. 6. Left: The residual deviation of the $(T - T_{90})_{meas}$ data listed in Tables 1 and 2 from the 12th-order fit function $D(T_{90})$ is shown versus temperature. WG4 is the data contained in Table 2 of Ref. 8 and shown for comparison purposes. The red dashed lines envelop the range $\pm u_{combined}[D(T_{90})]$ with the combined standard uncertainty $u_{combined}[D(T_{90})]$. Right: The same as on the left but in a restricted temperature range.

To investigate the effects of correlations, generalized least-squares fits with non-diagonal covariance matrices were performed. It was found that the fit uncertainties were insensitive to modest correlations and unreasonably large correlations were required to yield any significant effects. Therefore, the effects of correlations are assumed to be negligible.

The second contribution to the uncertainty, $u(T - T_{90})_{TPW}$, arises from the fact that most of the measurements of $(T - T_{90})$ used the TPW as a reference, and the uncertainty in the thermodynamic temperature of the TPW, $u(T_{TPW})$, is now 0.10 mK. Consequently, this uncertainty must be propagated to other temperatures by multiplying $u(T_{TPW})$ by the ratio T/T_{TPW} and adding in quadrature to the fit uncertainty. Note that the best estimate of the thermodynamic temperature of the triple point of water remains 273.1600(1) K, and readers who wish to use the triple point of water as a thermodynamic reference point should continue to use this value and uncertainty.

The third contribution is the non-uniqueness of the ITS-90, $u(T_{90})_{NU}$. It consists of different sub-contributions. In the present work, the dominant one is by nature a component that cannot be reduced. It is an inherent feature of the ITS-90 itself and not of the individual standard platinum resistance thermometer as the interpolation instrument. The complete input from Table 2 and part of the input from Table 1 already include the non-uniqueness component. For the present $(T - T_{90})$ data, this component is a clear and omnipresent Type B component and cannot be reduced by averaging different results as in this case for a fit to different datasets. It is clearly visible in Table 4 that, for temperatures below 25 K and above 255 K, the uncertainty of the fit $u_{fit}[D(T_{90})]$ is below $u(T_{90})_{NU}$. Consequently, to avoid underestimation of the overall uncertainty, it is preferable to allow for a potential double counting in some cases because the size of a possible overestimation is acceptable. Below 25 K, the estimates for the non-uniqueness are based on the standard deviation of the results obtained in Key Comparisons CCT-K1[49] and

TABLE 4. The fitting function $(T - T_{90})$ versus T_{90}, $D(T_{90})$, is tabulated at the same temperatures as in Ref. 8. In the next column, uncertainty of the weighted fit $u_{fit}[D(T_{90})]$ is listed. The following columns give the contributions that must be added to $u_{fit}[D(T_{90})]$ to give finally $u[D(T_{90})]$ as a combined uncertainty estimate for $D(T_{90})$. The $u_{combined}[D(T_{90})]$ values can be accessed in fitted form by the power series of sixth order $\{u_{combined-LS}[D(T_{90})]\}$ using the coefficients β_i given in Table 3

T (K)	$D(T_{90})$ (mK)	$u_{fit}[D(T_{90})]$ (mK)	$u(T - T_{90})_{TPW}$ (mK)	$u(T_{90})_{NU}$ (mK)	$u_{combined}[D(T_{90})]$ (mK)
4.2	0.00	0.06	0.00	0.12	0.13
5	0.07	0.05	0.00	0.12	0.13
6	0.16	0.03	0.00	0.12	0.12
7	0.22	0.03	0.00	0.12	0.12
8	0.27	0.03	0.00	0.12	0.13
9.288	0.32	0.04	0.00	0.12	0.13
11	0.36	0.04	0.00	0.14	0.15
13.8033	0.36	0.04	0.01	0.19	0.19
17.035	0.29	0.04	0.01	0.19	0.19
20.27	0.16	0.05	0.01	0.19	0.19
22.5	0.05	0.05	0.01	0.19	0.19
24.5561	−0.06	0.06	0.01	0.19	0.20
35	−0.76	0.10	0.01	0.24	0.26
45	−1.51	0.13	0.02	0.11	0.17
54.3584	−2.21	0.14	0.02	0.00	0.14
70	−3.30	0.14	0.03	0.07	0.15
77.657	−3.80	0.14	0.03	0.05	0.15
83.8058	−4.21	0.15	0.03	0.00	0.15
90	−4.62	0.15	0.03	0.05	0.16
100	−5.32	0.17	0.04	0.10	0.20
130	−7.30	0.21	0.05	0.16	0.27
161.405	−7.34	0.21	0.06	0.16	0.27
195	−4.73	0.18	0.07	0.12	0.23
234.3156	−2.89	0.10	0.09	0.00	0.13
255	−1.97	0.08	0.09	0.09	0.15
273.16	−0.07	0.07	0.10	0.00	0.12
290	2.29	0.09	0.11	0.18	0.23
302.9146	3.84	0.14	0.11	0.28	0.34
335	7.09	0.37	0.12	0.46	0.60

EURAMET.T-K1.1[50] in the temperature range from 4 to 25 K. From 25 to 335 K, recommendations of the CCT were considered that are given in Ref. 51.

The combination of the uncertainty components finally leads to the combined standard uncertainty $u[D(T_{90})]$ shown by the dashed lines in Fig. 6. Numerical values of the uncertainty are tabulated in Table 4 at the same temperatures as treated in Ref. 8. A polynomial of sixth order has also been fitted to the uncertainty estimates listed in Table 4 to give a simple smooth functional description. The coefficients are listed in Table 3.

The uncertainty $u[D(T_{90})]$ is the uncertainty in the correction $D(T_{90})$. To obtain the uncertainty of the thermodynamic temperature, this uncertainty must be added in quadrature to the uncertainty in users' realizations of ITS-90. Guidance on the realization of ITS-90 and on the calculation of the uncertainty can be found in the online BIPM guides.[52]

The function $D(T_{90})$ is valid in the range of the fitted data from 4 to 335 K, with a reduction in uncertainty of an order of magnitude compared to those given in Ref. 8. Users working in a broader temperature range above and below 335 K might be interested in a smooth correction. A smooth transition from the new function $D(T_{90})$ to the old WG4 fitting function for temperatures from the TPW up to the copper point, $D_{2011}(T_{90})$, deduced in Ref. 8, is the point of intersection at $T_{90} = 288.418$ K. $D_{2011}(T_{90})$ is given by

$$D_{2011}(T_{90})/\text{mK} = (T - T_{90})/\text{mK}$$
$$= (T_{90}/\text{K})\sum_{i=0}^{4} c_i (273.16 \text{ K}/T_{90})^{2i}, \quad (5)$$

with $c_0 = 0.0497$, $c_1 = -0.3032$, $c_2 = 1.0254$, $c_3 = -1.2895$, and $c_4 = 0.5176$ (for more details, see Ref. 8). In addition, the change of slope at the transition point is very small. If the user is only interested in the temperature range below 335 K, the new function $D(T_{90})$ is recommended.

5. Summary and Conclusions

Since 2011, when the previous estimates of $(T - T_{90})$ were published by the CCT, there has been a change in the definition of the kelvin, and significant advances in primary thermometry were achieved, yielding much improved measurements of $(T - T_{90})$ over the range from 4 to 323 K. The analysis here combines the new data with the older data used in the 2011 analysis to update the consensus values for $(T - T_{90})$ over the range from 4 to 323 K. The updated values are represented by a 12th-order polynomial (coefficients listed in Table 3) with uncertainties given by a sixth-order polynomial (Table 3). The uncertainties in the $(T - T_{90})$ values are now comparable with the uncertainty in the best primary measurements of thermodynamic temperatures and the uncertainties in ITS-90 realizations. Hence, in combination with ITS-90 measurements, the results presented here offer an important means for achieving a state-of-the-art determination of thermodynamic temperature without the high cost and inconvenience of primary thermometry.

For the temperature range below 4 K, the recommendations of Ref. 8 should be used. From 0.65 to 2 K, the application of the

helium-3 vapor-pressure scale PTB-2006[53] is recommended. This scale is consistent with the Provisional Low Temperature Scale of 2000, PLTS-2000,[54] from 0.65 to 1 K. From 2 to 4 K, the ITS-90 can be used. In this range, PTB-2006 and ITS-90 are equivalent. The recommendation is supported by a recently performed direct comparison of the melting and vapor pressures of helium-3 at the LNE.[55] A forthcoming overview[56] shows that the thermodynamic deviation of the ITS-90 below 1.5 K has been verified consistently in three different ways by two independent groups in each case.

6. Author Declarations

6.1. Conflict of interest

The authors have no conflicts to disclose.

7. Data Availability

Data sharing is not applicable to this article as no new data were created or analyzed in this study.

8. Appendix: Superseded Data Used in 2011 in Ref. 8

Table 5 contains the data used in 2011 in Ref. 8, which have now been superseded as discussed in Sec. 2.

TABLE 5. Dataset PTB_2011_org[19,20] listed here is superseded by PTB_2011_rev.[21] given in Table 1. The values are listed to allow for the complete reproduction of the values published in Ref. 8 (for details, see footnote b of Table 1)

T_{90} (K)	$(T - T_{90})$ (mK)	$u(T - T_{90})$ (mK)
4.2	0.04	0.17
5	0.24	0.18
6	0.10	0.19
7	−0.03	0.20
8	−0.04	0.20
9.288	0.04	0.22
11	0.14	0.23
13.8033	0.26	0.25
17.035	0.41	0.28
20.27	0.28	0.31
22.5	0.31	0.33
24.5561	0.42	0.35

9. References

[1] M. Stock, R. Davis, E. de Mirandés, and M. J. T. Milton, Metrologia **56**, 022001 (2019).

[2] E. O. Göbel and U. Siegner, *The New International System of Units (SI)* (Wiley-VCH, Berlin, 2019), ISBN: 978-3-527-34459-8.

[3] D. R. White, Contemp. Phys. **61**, 256 (2020).

[4] See https://www.bipm.org/en/publications/mises-en-pratique for the *Mise en pratique for the definition of the kelvin*.

[5] B. Fellmuth, J. Fischer, G. Machin, S. Picard, P. P. M. Steur, O. Tamura, D. R. White, and H. Yoon, Philos. Trans. R. Soc., A **374**, 20150037 (2016).

[6] H. Preston-Thomas, Metrologia **27**, 3 (1990); Erratum **27**, 107 (1990).

[7] B. Fellmuth, "Guide to the realization of the ITS-90. Part 1—Introduction," https://www.bipm.org/en/committees/cc/cct/guides-to-thermometry (2018).

[8] J. Fischer, M. de Podesta, K. D. Hill, M. Moldover, L. Pitre, R. Rusby, P. Steur, O. Tamura, R. White, and L. Wolber, Int. J. Thermophys. **32**, 12 (2011).

[9] See https://www.bipm.org/en/committees/cc/cct/temperature-scales for estimates of the differences between thermodynamic temperature and the ITS–90.

[10] B. Fellmuth, C. Gaiser, and J. Fischer, Meas. Sci. Technol. **17**, R145 (2006).

[11] J. Fischer, B. Fellmuth, C. Gaiser, T. Zandt, L. Pitre, F. Sparasci, M. D. Plimmer, M. de Podesta, R. Underwood, and G. Sutton, Metrologia **55**, R1 (2018).

[12] JCGM 100, "Evaluation of measurement data—Guide to the expression of uncertainty in measurement," https://www.bipm.org/en/committees/jc/jcgm/publications (2008).

[13] G. Benedetto, R. M. Gavioso, R. Spagnolo, P. Marcarino, and A. Merlone, Metrologia **41**, 74 (2004).

[14] L. Pitre, M. R. Moldover, and W. L. Tew, Metrologia **43**, 142 (2006).

[15] M. R. Moldover, S. J. Boyes, C. W. Meyer, and A. R. H. Goodwin, J. Res. Natl. Inst. Stand. Technol. **104**, 11 (1999).

[16] D. C. Ripple, G. F. Strouse, and M. R. Moldover, Int. J. Thermophys. **28**, 1789 (2007).

[17] G. F. Strouse, D. R. Defibaugh, M. R. Moldover, and D. C. Ripple, in *Temperature: Its Measurement and Control in Science and Industry*, edited by D. C. Ripple (AIP, Melville, NY, 2003), Vol. 7; AIP Conf. Proc. **684**, 31 (2003).

[18] M. B. Ewing and J. P. M. Trusler, J. Chem. Thermodyn. **32**, 1229 (2000).

[19] H. Luther, K. Grohmann, and B. Fellmuth, Metrologia **33**, 341 (1996).

[20] C. Gaiser, B. Fellmuth, and N. Haft, Int. J. Thermophys. **29**, 18 (2008).

[21] C. Gaiser, B. Fellmuth, and N. Haft, Metrologia **54**, 141 (2017).

[22] D. N. Astrov, L. B. Belyansky, and Y. A. Dedikov, Metrologia **32**, 393 (1995).

[23] P. P. M. Steur and M. Durieux, Metrologia **23**, 1 (1986).

[24] O. Tamura, S. Takasu, T. Nakano, and H. Sakurai, Int. J. Thermophys. **29**, 31 (2008).

[25] R. C. Kemp, W. R. G. Kemp, and L. M. Besley, Metrologia **23**, 61 (1986).

[26] K. H. Berry, Metrologia **15**, 89 (1979).

[27] R. M. Gavioso, D. Madonna Ripa, P. P. M. Steur, R. Dematteis, and D. Imbraguglio, Metrologia **56**, 045006 (2019).

[28] K. Zhang, X. J. Feng, J. T. Zhang, Y. Y. Duan, H. Lin, and Y. N. Duan, Metrologia **57**, 024004 (2020).

[29] R. Underwood, M. de Podesta, G. Sutton, L. Stanger, R. Rusby, P. Harris, P. Morantz, and G. Machin, Int. J. Thermophys. **38**, 44 (2017).

[30] V. G. Kytin, G. A. Kytin, M. Yu Ghavalyan, B. G. Potapov, E. G. Aslanyan, and A. N. Schipunov, Int. J. Thermophys. **41**, 88 (2020).

[31] C. Pan, F. Sparasci, H. Zhang, P. Gambette, M. Plimmer, D. Imbraguglio, R. M. Gavioso, M. R. Moldover, B. Gao, and L. Pitre, Metrologia **58**, 045006 (2021).

[32] J. V. Widiatmo, T. Misawa, T. Nakano, and I. Saito, Int. J. Thermophys. **41**, 42 (2020).

[33] C. Gaiser, B. Fellmuth, and N. Haft, Metrologia **57**, 055003 (2020).

[34] C. Gaiser and B. Fellmuth, Metrologia **58**, 042101 (2021).

[35] P. M. C. Rourke, Metrologia **57**, 024001 (2020).

[36] D. Madonna Ripa, D. Imbraguglio, C. Gaiser, P. P. M. Steur, D. Giraudi, M. Fogliati, M. Bertinetti, G. Lopardo, R. Dematteis, and R. M. Gavioso, Metrologia **58**, 069501 (2021).

[37] B. Gao, H. Zhang, D. Han, C. Pan, H. Chen, Y. Song, W. Liu, J. Hu, X. Kong, F. Sparasci, M. Plimmer, E. Luo, and L. Pitre, Metrologia **58**, 059501 (2021).

[38] T. Nakano, T. Shimazaki, and O. Tamura, Int. J. Thermophys. **38**, 105 (2017).

[39] P. J. Mohr, D. B. Newell, B. N. Taylor, and E. Tiesinga, Metrologia **55**, 125 (2018).

[40] Å. Björck, BIT Numer. Math. **7**, 1 (1967).

[41] Å. Björck, *Numerical Methods for Least Squares Problems* (Society for Industrial and Applied Mathematics, 1996).

[42] P. Saunders, Callaghan Innovation Report No. 18 (5.3), 2016.

[43] P. Saunders, Metrologia **40**, 93 (2003).

[44] W. H. Press, S. A. Teukolsky, W. T. Vetterling, and B. P. Flannery, *Numerical Recipes: The Art of Scientific Computing*, 3rd ed. (Cambridge University Press, 2007).

[45] R. L. Powell, W. J. Hall, and J. G. Hust, in *Temperature: Its Measurement and Control in Science and Industry*, edited by H. H. Plumb (Instrument Society of America, Pittsburgh, 1972), Vol. 4, p. 1423.

[46] K. P. Burnham and D. R. Anderson, Sociol. Methods Res. **33**, 261 (2004).

[47] R. L. Rusby, Int. J. Thermophys. **31**, 1567 (2010).

[48] L. Crovini, H. J. Jung, R. C. Kemp, S. K. Ling, B. W. Mangum, and H. Sakurai, Metrologia **28**, 317 (1991).

[49] R. Rusby, D. Head, C. Meyer, W. Tew, O. Tamura, K. D. Hill, M. de Groot, A. Storm, A. Peruzzi, and B. Fellmuth, Metrologia **43**, 03002 (2006).

[50] C. Gaiser, B. Fellmuth, P. Steur, A. Szmyrka-Grzebyk, H. Manuszkiewicz, L. Lipinski, A. Peruzzi, R. Rusby, and D. Head, Metrologia **54**, 03002 (2017).

[51] A. I. Pokhodun, B. Fellmuth, J. V. Pearce, R. L. Rusby, P. P. M. Steur, O. Tamura, W. L. Tew, and D. R. White, "Guide to the realization of the ITS-90: Chapter 5: Platinum resistance thermometry," https://www.bipm.org/en/committees/cc/cct/guides-to-thermometry (2018).

[52] See https://www.bipm.org/en/committees/cc/cct/guides-to-thermometry for guides to thermometry.

[53] J. Engert, B. Fellmuth, and K. Jousten, Metrologia **44**, 40 (2007).

[54] R. L. Rusby, M. Durieux, A. L. Reesink, R. P. Hudson, G. Schuster, M. Kühne, W. E. Fogle, R. J. Soulen, and E. D. Adams, J. Low Temp. Phys. **126**, 633 (2002).

[55] C. Pan, F. Sparasci, M. Plimmer, L. Risegari, J.-M. Daugas, G. Rouille, B. Gao, and L. Pitre, Metrologia **58**, 025005 (2021).

[56] B. Fellmuth and C. Gaiser, "Establishment and corroboration of a thermodynamically consistent Helium 3 vapour-pressure scale," Metrologia (to be published) (2023).

[57] M. S. Levenson, D. L. Banks, K. R. Eberhardt, L. M. Gill, W. F. Guthrie, H. K. Liu, M. G. Vangel, J. H. Yen, and N. F. Zhang, J. Res. Natl. Inst. Stand. Technol. **105**, 571 (2000).